Int. J. Heat Mass Transfer. Vol. 32, No. 2, pp. 311–319, 1989
Printed in Great Britain

0017–9310/89 $3.00 + 0.00

Effect of fiber orientation on thermal radiation in fibrous media

S. C. LEE
Thermal Control Department, The Aerospace Corporation, El Segundo, CA 90245, U.S.A.

(*Received* 4 *April* 1988 *and in final form* 17 *June* 1988)

Abstract—A radiation model is developed to evaluate the effect of fiber orientation on the radiative heat transfer through fibrous media between parallel planar diffuse boundaries. Fibers in the medium can be oriented in any given polar and azimuthal directions. Pertinent parameters in the model are the absorption ratio and the backscatter factor, which characterize the effect of the absorption coefficient and the amount of backscattered radiation, respectively. The analysis reveals that the polar orientation of the fibers strongly affects both the backscatter factor and radiative heat transfer. Radiative heat transfer is, however, independent of the azimuthal direction of the fibers. For fibers oriented parallel to the boundaries, backscattering of radiation is highest which results in minimum radiative heat transfer. If the fibers are oriented perpendicular to the boundaries, there is no backscattering of radiation and radiative heat transfer is affected only by the absorption coefficient. This then results in the highest radiative heat transfer.

INTRODUCTION

FIBROUS materials are commonly used as thermal insulation in many engineering systems due to their effectiveness in reducing the radiative heat transfer. Under atmospheric conditions fibers in the medium also suppress convection; therefore radiation and conduction heat transfer are both important even at the moderate temperatures of about 300–400 K [1–3]. Reduction of thermal radiation through these materials is therefore critical in improving their insulation capacity.

Radiation through fibrous media has been the subject of many recent investigations [4–10]. The analytical consideration ranged from the earlier empirical models to the recent more rigorous approaches. In the latter analyses fibers were modeled as infinitely long circular cylinders the radiation properties of which, e.g. the extinction and scattering coefficients, were calculated by using well-established formulae from electromagnetic theory [11, 12].

Radiative heat transfer through fibers oriented randomly in space had been considered in several studies [5, 7, 8]. The formulation for the radiative properties of fibrous media with any fiber orientation was derived in ref. [9]. In addition, the solution on the radiative transfer of collimated irradiation was presented for the case of fibers oriented normal to the incident irradiation. A radiative heat transfer model was also developed for fibrous media with fibers oriented parallel to planar boundaries [10].

Fibers in many insulation materials are neither randomly oriented in space nor oriented in planes. Instead they may be preferentially oriented in specific polar and/or azimuthal directions. It is necessary to be able to evaluate the effect of fiber orientation on the thermal insulation effectiveness of the fibrous medium in order to determine both the optimal fiber orientation and the penalty on the thermal insulation capacity due to deviation from the optimal fiber orientation. However, no analysis has yet been developed which can account for any fiber orientation in radiative heat transfer calculations.

This paper presents a radiation model applicable to fibrous media with any spatial orientation of fibers based on the two-flux approximation. The analytical formulation utilizes the previously derived transformations between the fiber and the global coordinate systems [9], as well as the radiation model for fibers oriented in planes [10]. For completeness and continuity, a brief review of the previous formulation is also included. This is followed by the analytical formulation to treat the general case of any fiber orientation. Numerical results will be shown to demonstrate the effect of fiber orientation on radiative heat transfer.

FORMULATION

Consider a medium of fibers contained between parallel diffuse boundaries. The boundaries are at temperatures T_1 and T_2 with diffuse emissivities ε_1 and ε_2, respectively. The equation of transfer can be written separately in terms of the radiative intensities traversing in the forward (I^+) and backward (I^-) directions as [10]

$$I^+: \quad \mu\frac{\mathrm{d}I^+}{\mathrm{d}y} = -KI^+ + \sigma_a I_b + [\sigma_s - B]I^+ + BI^-, \qquad 0 < \mu \leqslant 1 \quad (1a)$$

$$I^-: \quad \mu\frac{\mathrm{d}I^-}{\mathrm{d}y} = -KI^- + \sigma_a I_b + BI^+ + [\sigma_s - B]I^-, \qquad -1 \leqslant \mu < 0 \quad (1b)$$

NOMENCLATURE

B	backscatter parameter
$\bar{B}$	backscatter factor
d^2F	fiber orientation distribution function
e_1, e_2	Planck functions at the boundaries
i	unit intensity function
I^+	radiative intensity traversing in the forward hemisphere
I^-	radiative intensity traversing in the backward hemisphere
I_b	blackbody intensity
j	$\sqrt{-1}$
k	imaginary part of **m**
K	extinction coefficient
$\bar{K}$	average extinction coefficient, defined by equation (6) or (7)
L	depth of medium
m	complex index of refraction, $n-jk$
M	total number of weave directions
n	real part of **m**
$N(r)$	fiber number size distribution
q	radiative heat flux
Q	efficiency
r	radius of fiber
R	unit vector
x_j	fraction of fibers oriented in the jth direction
y	depth along medium.

Greek symbols

α	size parameter, $2\pi r/\lambda$
β_a	absorption ratio, $\bar{\sigma}_a/\bar{K}$
ε	surface emissivity
θ	angle of observation
θ_c	limit of integration for the backscatter parameter
λ	wavelength
μ	$\cos\xi$
ξ	polar angle
η	angle between the incident and scattered radiation
σ_a	absorption coefficient
$\bar{\sigma}_a$	average absorption coefficient, defined by equation (6) or (7)
σ_s	scattering coefficient
$\bar{\sigma}_s$	average scattering coefficient, defined by equation (6) or (7)
ϕ	angle of incidence
ϕ_c	complementary angle of incidence, $\lvert\pi/2-\phi\rvert$
ω	azimuthal angle.

Subscripts

a	absorption
e	extinction
f	fiber
i	incident radiation
j	$1, 2, \ldots, M$
m	medium
r	fibers randomly oriented in space
s	scattered radiation.

where K, σ_s, and σ_a are the extinction, scattering, and absorption coefficients, respectively, B the backscatter parameter, I_b the blackbody radiation, $\mu = (\cos\xi)$ the cosine of the polar angle ξ, and ω the azimuthal angle. The radiative coefficients and the backscatter parameter are, in general, functions of ξ and ω. Detailed discussion of these parameters will be given in the subsequent sections. Note that the radiative properties are angular dependent because the radiative cross sections of the fibers vary with the direction of the incident radiation [9]. All quantities in the above equations are spectral.

In the two-flux approximation the intensities I^+ and I^- are assumed to be isotropic in the respective hemispheres. By integrating equations (1a) and (1b) over the forward and backward hemispheres, respectively, and assuming radiative equilibrium, the net radiative heat flux can be obtained as [7, 10]

$$q = \int_0^\infty \frac{e_1 - e_2}{\left(\frac{1}{\varepsilon_1} + \frac{1}{\varepsilon_2} - 1\right) + (\beta_a - 2\bar{B})\bar{K}L}\,\mathrm{d}\lambda. \quad (2)$$

In the above equation e_1 and e_2 are the Planck function, λ the wavelength, L the thickness of the slab, $\beta_a = (\bar{\sigma}_a/\bar{K})$ the absorption ratio, $\bar{\sigma}_a$ and $\bar{K}$ the effective absorption and extinction coefficients, respectively, and $\bar{B}$ the backscatter factor. The backscatter factor $\bar{B}$ results from the hemispherical integration of the backscatter parameter B. A detailed derivation will be shown in a later section. Also, all quantities inside the integral are spectral and the subscript λ was omitted for clarity.

The absorption ratio and the backscatter factor are the pertinent parameters in the current radiation model. The derivation of these parameters had been presented for the specific case of fibers oriented parallel to the boundaries [10]. The formulation applicable for any fiber orientation is presented in the following sections. For continuity and clarity the transformation between the fiber and the global coordinates, as well as the formulation of the radiative properties of fibrous media with any fiber orientation are first briefly described.

Coordinate transformation

A fiber is modeled as an infinitely long circular cylinder because its length is generally much greater than both the wavelength of the radiation and the

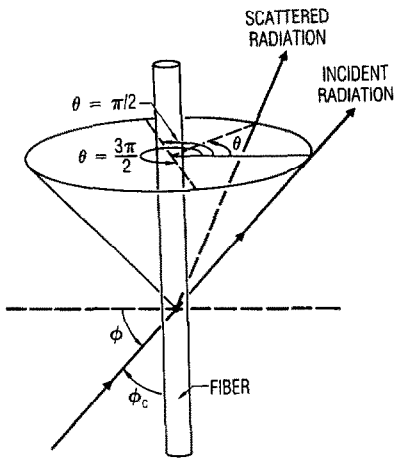

FIG. 1. Scattering of radiation by an infinite circular cylinder.

diameter of the fiber [5–10]. Figure 1 shows the scattering of radiation by a fiber at oblique incidence. The scattered radiation propagates along the surface of the cone with apex angle $\pi - 2\phi$, where ϕ is the angle of incidence measured from the normal of the fiber axis. The complementary angle of incidence ϕ_c is measured from the fiber axis. The angle between the incident and scattered radiation measured on the base of the cone is called the angle of observation θ. The angles θ, ϕ, and ϕ_c are defined relative to the coordinate system attached to the fiber.

Figure 2 depicts a fiber oriented between two planar boundaries that are located parallel to the X–Z plane. $\mathbf{R}_i$, $\mathbf{R}_s$, and $\mathbf{R}_f$ are unit vectors in the direction of the incident radiation, the scattered radiation, and the fiber axis, respectively. The fiber coordinates (θ, ϕ) are related to the global coordinates (ξ, ω) by [9]

$$\cos\phi_c = \sin\phi = \mathbf{R}_i \cdot \mathbf{R}_f = \mathbf{R}_s \cdot \mathbf{R}_f$$

$$= \sin\xi_i \sin\xi_f \cos(\omega_i - \omega_f) + \cos\xi_i \cos\xi_f \quad (3a)$$

$$= \sin\xi_s \sin\xi_f \cos(\omega_s - \omega_f) + \cos\xi_s \cos\xi_f \quad (3b)$$

where subscripts i, s, and f refer to the incident radiation, the scattered radiation, and the fiber, respectively. The included angle η and the angle of observation θ between the incident and the scattered radiation are related to $\mathbf{R}_i$, $\mathbf{R}_s$, and $\mathbf{R}_f$ by

$$\cos\eta = \mathbf{R}_i \cdot \mathbf{R}_s = \sin\xi_i \sin\xi_s \cos(\omega_i - \omega_s) + \cos\xi_i \cos\xi_s \quad (4a)$$

$$\cos\theta = [(\mathbf{R}_i - \mathbf{R}_f \sin\phi) \cdot (\mathbf{R}_s - \mathbf{R}_f \sin\phi)]/\cos^2\phi$$

$$= (\cos\eta - \sin^2\phi)/\cos^2\phi. \quad (4b)$$

These transformations are used in the derivation of the radiative properties in the subsequent sections. The subscript i associated with the coordinates of the incident radiation will be omitted for brevity.

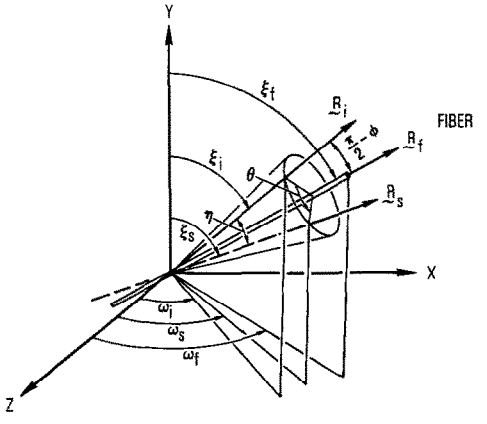

FIG. 2. Fiber orientation in space (boundaries parallel to the X–Z plane).

Radiative properties

Expressions for the extinction and scattering efficiencies $\{Q_e(\phi)$ and $Q_s(\phi)\}$ and the unit intensity distribution function $i(\theta, \phi)$ for a single fiber are well established [11, 12]. These quantities are wavelength dependent which are functions of both the refractive index and the fiber size. The radiative coefficients for a medium of fibers are obtained by integrating the respective efficiencies for the fibers over the size and orientation distributions [9]. By using the coordinate transformations given by equations (3a) and (3b), the radiative coefficients relative to the radiation traversing in the direction of (ξ, ω) are calculated by

$$\{K, \sigma_s, \sigma_a\} = \int_{\omega_{f1}}^{\omega_{f2}} \int_{\xi_{f1}}^{\xi_{f2}} \int_0^\infty 2r\{Q_e, Q_s, Q_a\} \times N[r(\mathbf{R}_f)]\, dr\, d^2F \quad (5)$$

where $Q_a = (Q_e - Q_s)$ is the absorption efficiency, and d^2F and $N(r)\, dr$ are the orientation distribution and number size distribution functions for the fibers, respectively. The limits of integration $(\xi_{f1}, \xi_{f2}, \omega_{f1}, \omega_{f2})$ denote the range of the angular orientation of the fibers. Typical variations of the radiative coefficients with the direction of the incident radiation and the fiber orientation were shown in ref. [9]. If the fibers are randomly oriented in space, the radiative coefficients become [9]

$$\{\bar{K}, \bar{\sigma}_s, \bar{\sigma}_a\} = \int_0^\infty \int_0^{\pi/2} 2r\{Q_e, Q_s, Q_a\} \cos\phi\, d\phi\, N(r)\, dr \quad (6)$$

which are independent of angle.

An important result is obtained for the effective radiative coefficients in the two-flux approximation. These coefficients correspond to the average values over all the directions of the incident radiation. They are obtained by integrating equation (5) over a hemisphere as

$$\{\bar{K}, \bar{\sigma}_s, \bar{\sigma}_a\} = \frac{1}{2\pi} \int_0^{2\pi} \int_0^{\pi/2} \{K, \sigma_s, \sigma_a\} \sin\xi\, d\xi\, d\omega \quad (7)$$

which are independent of the fiber orientation. It can

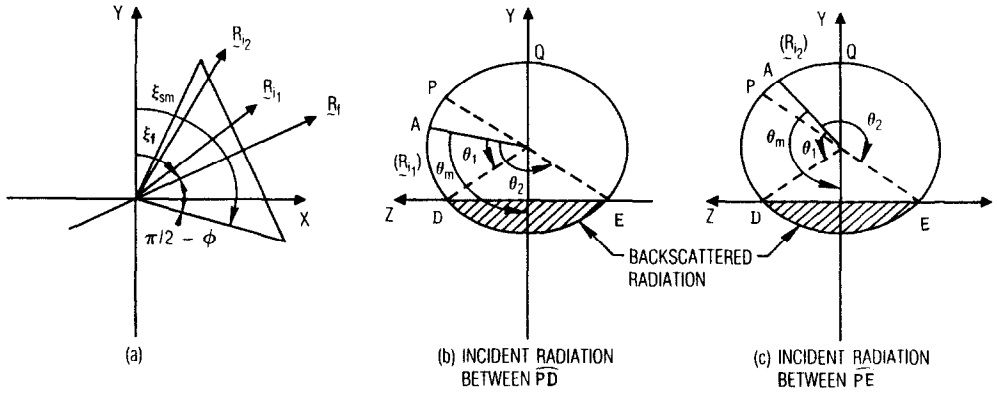

FIG. 3. Scattering geometry for $\omega_i - \omega_f < \pi/2$.

be readily shown that the radiative coefficients calculated by equations (6) and (7) are identical.

Backscatter parameter B and backscatter factor $\bar{B}$

The backscatter parameter B denotes the amount of radiation scattered by all fibers into a hemisphere due to the radiation traversing in a particular direction in the opposite hemisphere. It is therefore affected by both the direction of the incident radiation and the orientation of the fibers. The backscatter factor $\bar{B}$ corresponds to the total amount of radiation scattered into a hemisphere due to radiation traversing in all directions in the opposite hemisphere. It is obtained by integrating the backscatter parameter B over a hemisphere, as will be shown later.

The evaluation of B and $\bar{B}$ can be better understood by considering the scattering of a ray of radiation ($\mathbf{R}_i$) traversing in the upper hemisphere (i.e. $0 \leqslant \xi < \pi/2$, $0 \leqslant \omega < 2\pi$) by a fiber ($\mathbf{R}_f$) as depicted in Figs. 3–5. The side views of the cone of scattered radiation are shown in Figs. 3(a), 4(a), and 5(a), and the end views containing the projection of the base of the cone are shown in Figs. 3(b) (for $\mathbf{R}_{i1}$), 3(c) (for $\mathbf{R}_{i2}$), 4(b), and 5(b). In these figures point A on the base of the cone denotes the direction of the incident radiation. The cone of scattered radiation intersects the horizontal X–Z plane that contains the apex of the cone at points D and E. The portion of the cone confined below the horizontal plane corresponds to the backscattered radiation due to the incident radiation designated by $\mathbf{R}_i$. The angles of observation θ_1 and θ_2 are measured on the base of the cone from point A (i.e. the incident radiation) to points D and E, respectively. Their values depend on the relative directions of the incident radiation and the orientation of the fiber as given by equation (3b). For certain combinations of these directions, the cone would not intersect the horizontal plane as depicted in Fig. 4. In this case no radiation can be scattered into the hemisphere opposite to that containing the direction of the incident radiation.

The backscatter parameter B for fibers oriented in random azimuthal directions parallel to planar boundaries was previously derived as [10]

$$B(\mu;\xi_f=\pi/2)=\frac{\lambda}{2\pi^3}\int_0^{\infty}\int_0^{2\pi}\int_{\theta_1}^{\theta_1+\pi} i(\theta,\phi)\times\delta(\xi_f-\pi/2)\,d\theta\,d\omega_f\,N(r)\,dr. \quad (8)$$

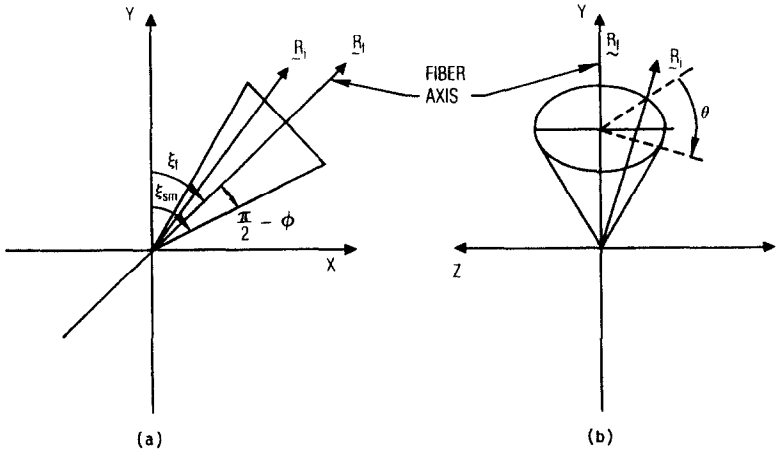

FIG. 4. Scattering geometry for no backscattered radiation.

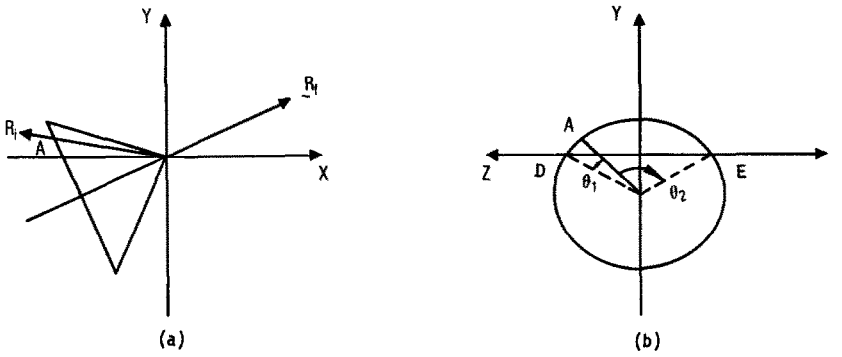

FIG. 5. Scattering geometry for $\omega_i - \omega_f \geqslant \pi/2$.

The coordinate transformations given by equations (3) and (4) are required in order to evaluate this expression. The backscatter parameter is independent of the azimuthal angle ω due to the integration over all azimuthal orientations of the fibers. The corresponding expression for fibers woven in specific azimuthal directions is

$$B(\mu, \omega; \xi_f = \pi/2) = \frac{\lambda}{2\pi^3} \sum_{j=1}^{M} x_j \int_{r(\mathbf{R}_f)} \int_{\theta_1}^{\theta_1+\pi} i(\theta, \phi) \times \delta(\xi_f - \pi/2)\delta(\omega_f - \omega_{fj})\, d\theta\, N[r(\mathbf{R}_f)]\, dr \quad (9)$$

where x_j is the fraction of fibers in the ω_{fj} direction. The dependence of B on the azimuthal direction ω results from the discrete weave directions of the fibers.

In general if all the fibers are oriented in the polar direction, ξ_{fk}, different from $\pi/2$, the backscatter parameter is obtained by replacing the polar angle inside the Dirac delta function by ξ_{fk}. The backscatter parameter for fibers randomly oriented in the azimuthal directions becomes

$$B(\mu; \xi_f = \xi_{fk}) = \frac{\lambda}{2\pi^3} \int_0^{\infty} \int_0^{2\pi} \int_{\theta_{c1}}^{\theta_{c2}} i(\theta, \phi) \times \delta(\xi_f - \xi_{fk})\, d\theta\, d\omega_f\, N(r)\, dr. \quad (10)$$

For fibers woven in specific azimuthal directions, the backscatter parameter is

$$B(\mu, \omega; \xi_f = \xi_{fk}) = \frac{\lambda}{2\pi^3} \sum_{j=1}^{M} x_j \int_{r(\mathbf{R}_f)} \int_{\theta_{c1}}^{\theta_{c2}} i(\theta, \phi) \times \delta(\xi_f - \xi_{fk})\delta(\omega_f - \omega_{fj})\, d\theta\, N[r(\mathbf{R}_f)]\, dr. \quad (11)$$

The angles θ_{c1} and θ_{c2} are measured between points A and D and points A and E, respectively, on the base of the cone of scattered radiation as shown in Figs. 3 and 5. The integration over θ_c is performed in the counter-clockwise direction. The θ_cs are related to the angles θ_1, θ_2, and θ_m. The dependence of θ_c on these angles will be presented in the subsequent section.

The backscatter parameter for fibers randomly oriented in space (B_r) is obtained by integrating equation (10) or (11) over the polar angles as

$$B_r = \int_0^{\pi/2} B(\mu, \omega; \xi_{fk}) \sin \xi_{fk}\, d\xi_{fk}. \quad (12)$$

The backscatter factor $\bar{B}$ denotes all the radiation scattered into a hemisphere due to radiation traversing in all directions in the opposite hemisphere. It is obtained by integrating the backscatter parameter B over a hemisphere and normalized by the effective extinction coefficient $\bar{K}$ as

$$\bar{B} = \int_0^{2\pi} \int_0^{\pi/2} B(\mu, \omega) \sin \xi\, d\xi\, d\omega / 2\pi \bar{K}. \quad (13)$$

The angles θ_c are functions of both the incident direction and fiber orientation. The particular combination of the directions of the fiber and the incident radiation dictates the values of θ_c. There is, in general, no definite angular relationship between θ_{c1} and θ_{c2}. The only exception is when the fibers are oriented in planes; these two angles then differ by π. The complicated dependence of θ_c on $\mathbf{R}_i$ and $\mathbf{R}_f$ necessitates a detailed consideration of the geometry of the scattering of radiation in the coordinate system relative to the boundaries. The derivation of the angles θ_c is described in the following section.

Determination of the angles θ_c

Figures 3–5 show the three basic geometries of the cone of scattered radiation by a fiber in the direction $\mathbf{R}_f$ due to radiation traversing in a forward direction. The coordinates of the unit vectors for the incident radiation, the scattered radiation, and the fiber are designated by (ξ, ω), (ξ_s, ω_s), and (ξ_f, ω_f), respectively. The criterion for backscattering to exist is that the maximum polar angle ξ_{sm} corresponding to the lowest edge of the cone of scattered radiation exceeds $\pi/2$. Otherwise, there is no backscattered radiation which is the case depicted in Fig. 4.

If the azimuthal direction of the incident radiation and the fiber axis are in the same quadrant, equation (3a) dictates that $\phi_c < \pi/2$. Figures 3 and 4 show the scattering geometries for this case. From simple geometric consideration, the maximum polar angle is equal to

$$\xi_{sm} = \xi_f + \frac{\pi}{2} - \phi. \tag{14}$$

If the entire cone of scattered radiation lies above the horizontal plane as shown in Fig. 4, then $\xi_{sm} < \pi/2$ and there is no backscattering of radiation.

Figures 3 and 5 depict the geometries when backscattering of radiation occurs. In these figures point A denotes the direction of the incident ray of radiation, and points D and E denote the locations at which the cone intersects the horizontal X–Z plane containing the apex of the cone. The coordinates of the scattered radiation traversing points D and E are $(\xi_s = \pi/2, \omega_{s1})$ and $(\xi_s = \pi/2, \omega_{s2})$, respectively. The portion of the cone between points D and E below the horizontal plane is the backscattered radiation.

For the case depicted in Fig. 3, $\omega - \omega_f < \pi/2$ which corresponds to $\phi_c < \pi/2$. The angles ϕ and ϕ_c are determined by equation (3a) for the particular combination of the directions of the incident radiation and fiber orientation. By using $\xi_s = \pi/2$, the azimuthal angles for points D and E are determined from equation (3b) as

$$\omega_s = \omega_f \pm \cos^{-1}\left\{\frac{\sin\phi}{\sin\xi_f}\right\}. \tag{15}$$

These two roots are substituted into equation (4a) to calculate the two corresponding values of $\cos\eta$ which are then used in equation (4b) to determine the two roots of θ.

Two different sets of θ_1 and θ_2 as shown in Figs. 3(b) and (c) result depending on whether the incident direction is between $\overline{PD}$ (Fig. 3(b)) or $\overline{PE}$ (Fig. 3(c)). The need to distinguish between these sets of values in the calculation of the backscatter parameter B can be avoided by using the lowest edge of the cone as the reference direction. This edge corresponds to the ray of scattered radiation the coordinates of which are given by (ξ_{sm}, ω_f). The angle θ_m is then obtained by substituting the coordinates (ξ_{sm}, ω_f) and (ξ, ω) for the scattered radiation and the incident radiation, respectively, into equations (4a) and (4b). Consequently, the limits to be used in the evaluation of the backscatter parameter are

$$\begin{aligned} \theta_{c1} &= \theta_1 \\ \theta_{c2} &= \theta_1 + 2(\theta_m - \theta_1) \end{aligned} \tag{16}$$

for $\omega - \omega_f < \pi/2$.

Figure 5 shows the case of $\omega - \omega_f \geqslant \pi/2$ which dictates that $\phi_c \geqslant \pi/2$. The angles ϕ and ϕ_c are again determined by equation (3a) for a given ray of radiation incident on a fiber. By using $\xi_s = \pi/2$, the azimuthal angles for points D and E are determined from equation (3b) as

$$\omega_s = \pi + \omega_f \pm \cos^{-1}\left\{\frac{\sin\phi}{\sin\xi_f}\right\}. \tag{17}$$

The corresponding θs at these two points are evaluated by using equations (4a) and (4b) for a given direction (ξ, ω) of the incident radiation. The limits to be used to evaluate the backscatter parameter are

$$\begin{aligned} \theta_{c1} &= \theta_1 \\ \theta_{c2} &= \theta_1 + \pi \end{aligned} \tag{18}$$

for $\omega - \omega_f \geqslant \pi/2$.

It is obvious from the above derivation that angles θ_c are different for each combination of the directions of the incident radiation and the fiber axis. The θ_cs given in equations (16) and (18) are used in equations (10) and (11) for evaluating the backscatter parameter B. Finally, the backscatter factor $\bar{B}$ for all the above cases is obtained by integrating the backscatter parameter B over the hemisphere of all directions of the incident radiation as given in equation (13).

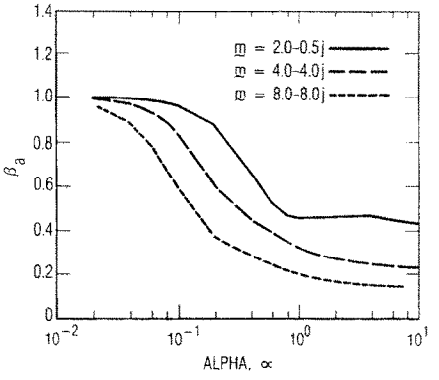

FIG. 6. Variation of the absorption ratio with size parameter.

RESULTS AND DISCUSSION

The effect of fiber orientation on the backscatter factor and radiative heat transfer for various fiber size parameters and optical properties are discussed in this section. The fibers are assumed to be inclined at specific polar angles, except for the case of fibers randomly oriented in space. For simplicity of illustration, the following assumptions are made: monosize fibers, gray radiative properties, and black boundaries. Three different refractive indices are used for demonstration.

Figure 6 shows the absorption ratio β_a as a function of the size parameter α for different refractive indices $\mathbf{m}$. Absorption dominates for small values of α and β_a approaches unity. As α increases, scattering becomes more significant and β_a decreases. Figure 7 shows the variation of the backscatter factor with the fiber size parameter for different fiber orientations. The backscatter factor is zero if the fiber axes are perpendicular to the boundaries, i.e. $\xi_f = 0$. This is physically obvious by observing the characteristics of the scattering of radiation by a fiber as depicted in Fig. 1. Considering the fiber axis in Fig. 1 to be normal to the boundaries, the scattered radiation is confined in the same hemisphere as the incident radiation. Hence, radiation cannot be scattered into the hemisphere opposite to that containing the incident radiation and

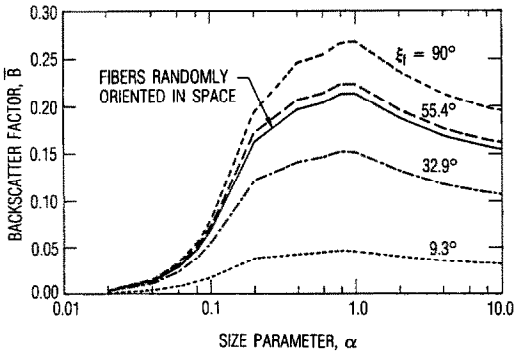

FIG. 7. Effect of the polar inclination of fibers on the backscatter factor.

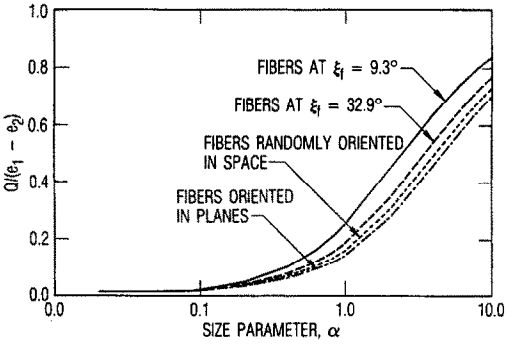

FIG. 9. Variation of the radiative heat flux with the fiber size parameter for $\mathbf{m} = 4.0-4.0\mathrm{j}$ and $f_v L/\lambda = 1.0$ between black boundaries ($f_v (= \pi r^2 lN)$ is the volume fraction, l the average length of a fiber, and N the number density of fibers).

the backscatter factor is zero. The backscatter factor increases as the polar inclination of the fibers increases. It is largest for fibers oriented parallel to the boundaries, i.e. $\xi_f = 90°$, and is lower for fibers randomly oriented in space. The maximum occurs when α is of the order of unity. Note that the backscatter factors for different types of fiber orientations converge and approach zero for small α. This is because scattering becomes negligible compared to absorption in this regime. Figure 8 shows that the backscatter factor increases with the refractive index. This is because the scattering coefficient becomes larger as the refractive index increases. The above results indicate that both the fiber size and fiber orientation are important parameters affecting the amount of backscattered radiation by a fibrous medium.

The effect of fiber orientation on radiative heat transfer through a fibrous medium is shown in Fig. 9. The most effective thermal insulation, i.e. lowest heat transfer, is obtained for fibers oriented parallel to the boundaries. The insulation capacity decreases as the fibers deviate from this orientation. In particular, the highest radiative heat transfer results for fibers oriented perpendicular to the boundaries. This is because the backscatter factor is zero and radiative heat transfer is governed only by the absorption coefficient. These results also indicate the penalty on the thermal performance due to different fiber orientations. Figure 10 shows the effect of refractive index $\mathbf{m}(= n-jk)$ on the radiative heat transfer. The effect of the optical properties is more pronounced when the polar inclination of the fibers is small. For the refractive indices used in the present study, the effect of the absorption ratio is more dominant than the backscatter factor. Hence, radiative heat transfer is higher for the larger refractive index. For typical fiberglass insulation, n is much higher than k and the effect of fiber orientation will be more pronounced when realistic optical properties are employed.

The above results reveal that the scattering coefficient alone is not sufficient to characterize the radiative heat transfer through fibrous media. This is because the distribution of the scattered intensity varies with the spatial orientation of the fibers and the direction of the incident radiation. Fiber orientation is a critical factor that dictates the magnitude of the backscatter factor.

The proper definition of radiation backscattering is very important in the calculation of radiative heat transfer through fibrous media. For scattering of radiation by fibers, the backscattering of radiation relative to a single fiber should be distinguished from the backscattering with respect to the boundaries. In the former case backscattering simply refers to the

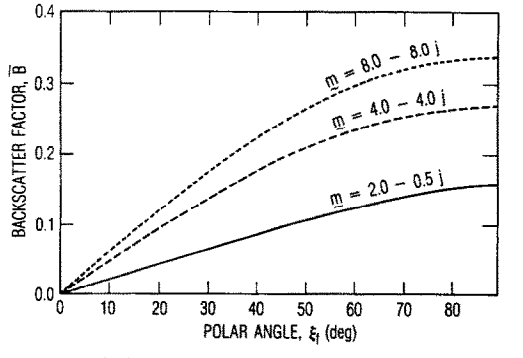

FIG. 8. Variation of the backscatter factor with size parameter for fibers oriented in specific polar angles ($\mathbf{m} = 4.0-4.0\mathrm{j}$). $\alpha = 1.0$.

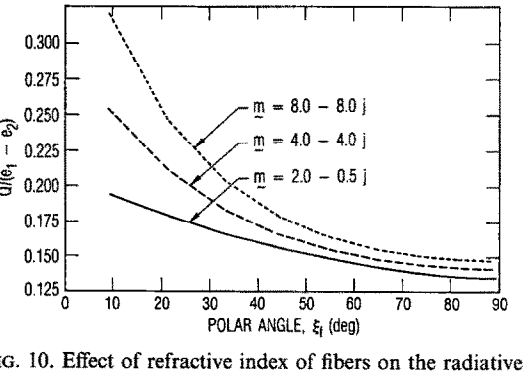

FIG. 10. Effect of refractive index of fibers on the radiative heat transfer for fibers oriented in various polar angles for $f_v L/\lambda = 1.0$ ($f_v (= r^2 lN)$ is the volume fraction, l the average length of a fiber, and N the number density of fibers).

portion of scattered radiation confined between the region $\pi/2 \leqslant \theta \leqslant 3\pi/2$ as shown in Fig. 1. Backscattering relative to the boundaries refers to the radiation scattered into the opposite hemisphere from that containing the incident direction. Depending on how the fibers are oriented relative to the boundaries, none or only part of the scattered radiation by each fiber would contribute to the backscattered radiation relative to the boundaries. In the previous radiation models [5, 7], no distinction was made between these two types of backscattering of radiation. The inadequate assumption can result in considerable uncertainties in these models as was pointed out in ref. [10].

It should be emphasized that the backscatter parameter in the present model is derived based on the phase function for a single fiber. This phase function is defined in terms of the natural coordinate system (θ, ϕ) of a fiber [10]. The alternative approach is to use the effective phase function of a medium which has been integrated over the fiber orientation distribution for the specific type of fiber orientation [9]. Hence, a specific phase function is associated with the corresponding type of fiber orientation. For the case of fibers randomly oriented in space, Houston and Korpela [8] expanded that specific phase function in terms of Legendre polynomials. The resulting series contains 20 terms in the far infra-red and 60 terms in the near infra-red. Each type of fiber orientation requires a similar series expansion with at least as many terms. Developing series expansions for each type of fiber orientation and including them in any numerical computation is a formidable task. However, the present approach of using the phase function defined relative to a single fiber circumvents the need to derive specific series expansions for the phase function of each type of fiber orientation. This approach of considering the physical geometry of the radiation scattered by each fiber avoided the mathematical complexity that would result if the phase function of a medium is used. This approach greatly facilitates numerical computations.

CONCLUSION

A radiation model applicable to fibrous media with any spatial fiber orientation was developed to evaluate the effect of fiber orientation on radiative heat transfer. Pertinent parameters in the model are the absorption ratio and the backscatter factor. The orientation of fibers was shown to strongly affect the thermal insulation characteristics of a fibrous medium.

The importance of fiber orientation is manifested by the limiting case of fibers all oriented perpendicular to the boundaries. In this case there is no backscattering of radiation, regardless of the magnitude of the scattering coefficient. Radiative heat transfer is then governed solely by the absorption coefficient. Backscattering gradually increases as the fiber axes deviate from the perpendicular position. This indicates that fiber orientation is indeed an important parameter affecting radiative heat transfer through a fibrous medium.

The present radiation model uses the two-flux approximation which generally becomes less accurate when the radiation intensity deviates from the isotropic distribution. This approach is nevertheless useful for engineering estimates due to its simplicity. Since the geometry of the scattered radiation was considered in detail, the current formulation can easily be extended to a multi-flux model should a higher degree of accuracy be desired.

REFERENCES

1. J. D. Verschoor and P. Greebler, Heat transfer by gas conduction and radiation in fibrous insulation, *ASME Trans.* **74,** 961–968 (1952).
2. C. G. Bankvall, Heat transfer in fibrous materials, *J. Test. Eval.* **1,** 235–243 (1973).
3. C. M. Pelanne, Heat flow principles in thermal insulations, *J. Ther. Insul.* **1,** 48–80 (1977).
4. T. W. Tong and C. L. Tien, Analytical models for thermal radiation in fibrous insulations, *J. Ther. Insul.* **4,** 27–44 (1980).
5. T. W. Tong and C. L. Tien, Radiative heat transfer in fibrous insulations—Part I: analytical study, *J. Heat Transfer* **105,** 70–75 (1983).
6. T. W. Tong and C. L. Tien, Radiative heat transfer in fibrous insulations—Part II: experimental study, *J. Heat Transfer* **105,** 70–75 (1983).
7. K. Y. Wang and C. L. Tien, Radiative transfer through opacified fibers and powders, *J. Quant. Spectrosc. Radiat. Transfer* **30**(3), 213–223 (1983).
8. R. L. Houston and S. A. Korpela, Heat transfer through fiberglass insulation, *Proc. 7th Int. Heat Transfer Conf.*, Vol. 2, pp. 499–504 (1982).
9. S. C. Lee, Radiative transfer through a fibrous medium: allowance for fiber orientation, *J. Quant. Spectrosc. Radiat. Transfer* **36**(3), 253–263 (1986).
10. S. C. Lee, Radiation heat transfer model for fibers oriented parallel to diffuse boundaries, *J. Thermophys. Heat Transfer* **2**(4), 303–308 (1988).
11. H. C. Van de Hulst, *Light Scattering by Small Particles*. Chap. 15. Dover, New York (1981).
12. M. Kerker, *The Scattering of Light and other Electromagnetic Radiation*, Chap. 6. Academic Press, New York (1969).

EFFET DE L'ORIENTATION DES FIBRES SUR LE RAYONNEMENT THERMIQUE DANS LES MILIEUX FIBREUX

Résumé—Un modèle de rayonnement est développé pour évaluer l'effet de l'orientation des fibres sur le transfert radiatif à travers des milieux fibreux entre des frontières planes, parallèles et diffusantes. Les fibres peuvent être orientées dans des directions polaires et azimutales quelconques. Les paramètres pertinents du modèle sont le rapport d'absorption et le facteur de rétrodiffusion qui caractérisent respectivement l'effet du coefficient d'absorption et celui du rayonnement rétrodiffusé. L'analyse montre que l'orientation polaire des fibres affecte fortement à la fois le facteur de rétrodiffusion et le transfert radiatif. Celui-ci est néanmoins indépendant de la direction azimutale des fibres. Pour les fibres orientées parallèlement aux frontières, la rétrodiffusion est plus élevée ce qui rend minimal le transfert par rayonnement. Si les fibres sont orientées perpendiculairement aux frontières, il n'y a pas de rétrodiffusion et le transfert radiatif est affecté seulement par le coefficient d'absorption. Ceci provoque alors le transfert radiatif maximal.

EINFLUSS DER FASER-OPTIMIERUNG AUF DEN STRAHLUNGSWÄRMEAUSTAUSCH IN FASERIGEN STOFFEN

Zusammenfassung—Es wurde ein Modell zur Bestimmung des Einflusses der Faser-Orientierung auf den Strahlungswärmeaustausch in faserigen Stoffen zwischen planparallelen, diffus reflektierenden Grenzflächen entwickelt. Die Fasern können in allen Richtungen orientiert sein. Maßgebende Modell-Parameter sind das Absorptionsverhältnis und der Faktor der Rückströmung, welche den Einfluß des Absorptionskoeffizienten und den Betrag der rückreflektierten Strahlung charakterisieren. Die Untersuchung zeigt, daß die polare Orientierung der Fasern sich stark auf den Rückstreufaktor und den Strahlungswärmeaustausch auswirkt. Der Azimutwinkel beeinflußt den Strahlungswärmeaustausch nicht. Für eine zu den Grenzflächen parallele Faser-Orientierung wird die Rückstreuung am größten, was zu einem Minimum im Strahlungsaustausch führt. Bei senkrechter Faser-Orientierung tritt keine Rückstreuung auf, so daß der Strahlungsaustausch nur vom Absorptionskoeffizienten abhängt. Dies führt zum höchsten Strahlungswärmeaustausch.

ВЛИЯНИЕ ОРИЕНТАЦИИ ВОЛОКНА НА ТЕПЛОВОЕ ИЗЛУЧЕНИЕ В ПОРИСТЫХ СРЕДАХ

Аннотация—Разработана модель теплового излучения для оценки влияния ориентации волокна на радиационный теплоперенос в волокнистых средах между параллельными плоскими диффузными границами. Волокна могут быть ориентированы в полярном или азимутальном направлениях. Типичными для данной модели параметрами являются коэффициенты поглощения и обратного рассеяния. Анализ показал, что полярная ориентация волокон сильно влияет на коэффициент обратного рассеяния и радиационный теплоперенос, в то время как от азимутального направления волокон радиационный теплоперенос не зависит. Обратное рассеяние излучения наиболее интенсивно при ориентации волокон параллельно границам, что снижает радиационный теплоперенос до минимума. В случае, когда волокна направлены перпендикулярно к границам, обратное рассеяние излучения отсутствует, и радиационный теплопренос зависит только от коэффициента поглощения, в результате чего интенсивность радиационного теплопереноса максимально повышается.